# Parametric study on propulsion performance of micro-tubes

Christos Tantos and Dimitris Valougeorgis

Dept. of Mechanical Engineering, University of Thessaly, Laboratory of Transport Phenomena

Pedion Areos, 38334 Volos, Greece

#### **Abstract**

The pressure driven rarefied gas flow of polyatomic gases through short tubes in a wide range of the Knudsen number is numerically investigated. The downstream over the upstream pressure ratio is taken very close to zero. Such flows are characterized by low Reynolds numbers and high viscous losses and therefore short circular micro-tubes may be used instead of typical micro-nozzles. The main computed quantities include the flow rate, the discharge coefficient, the thrust and the impulse factor which are provided in terms of the gas rarefaction and the tube dimensionless length. Based on the above a parametric study on the propulsion characteristics of micro-tubes is provided. Furthermore, a comparison between corresponding polyatomic and monatomic results is performed and the effect of the internal degrees of freedom on the results is investigated.

#### 1. Introduction

In several practical applications including micro propulsion nozzles in high altitude the flow may be in the whole range of the Knudsen number and modelling must be based on deterministic techniques solving the Boltzmann equation or alternatively on the stochastic DSMC method. Micro-nozzles are often used as low-thrust propulsion systems in order to produce accurate orbital maneuvers in micro-satellites. Therefore, a systematic study of the gas flow in such devices is needed in order to determine the optimal geometry and design. It is well known that, at low Reynolds numbers, the viscous losses in micronozzles become large enough making the concept of a nozzle expansion useless and micronozzles can be replaced by short circular tubes. Rarefied monatomic gas flows through capillaries due to pressure gradients have been extensively studied in the past [1, 2, 3]. The corresponding work in polyatomic gases is commonly handled based on the DSMC method, while similar simulations based on kinetic modelling are limited.

In the present work the rarefied gas flow of polyatomic gases through short circular tubes due to pressure gradients is modelled via the polyatomic Holway model of the Boltzmann equation [4]. This model holds the entropy inequality and ensures good agreement with experimental data concerning heat transfer [5, 6] and steady condensation [7] configurations. The purpose of the present work is to numerically investigate polyatomic gas expansion into very low pressures in a wide range of the Knudsen number and to compute the deduced flow rate, discharge coefficient, thrust the impulse factor in terms of flow and geometric parameters as well as to examine the effect of the internal degrees of freedom by comparison with corresponding monatomic flows.

## 2. Flow configuration and basic parameters

Consider two large reservoirs A and B which are connected by a tube of radius R and finite length L. The polyatomic gas in the containers far from the tube is in equilibrium at pressures  $P_A$  and  $P_B$ , with  $P_B/P_A=0.01$ . The walls and the gas in the container areas far from the tube are maintained at the same temperature  $T_0$ . The computational domain consists of the two large computational areas, which correspond to the upstream and downstream reservoir including an intermediate area which contains the tube. The flow configuration and the computational domain are shown in Fig. 1. The reference quantities are R,  $T_0$  and  $P_A$ , while the most probable speed, defined as  $v_0 = \sqrt{2k_BT_0/m}$  with m and  $k_B$  denoting the molecular mass and the Boltzmann constant respectively, is taken as the reference velocity. The flow is characterized by the ratio L/R and the rarefaction parameter defined as

$$\delta_0 = \frac{P_A R}{\mu_0 \nu_0} \tag{1}$$

where  $\mu_0$  is the reference viscosity at temperature  $T_0$ . It is noted that the rarefaction parameter is proportional to the inverse Knudsen number, with the limiting values at  $\delta_0 = 0$  and  $\delta_0 \to \infty$  corresponding to the free molecular and hydrodynamic limits respectively.

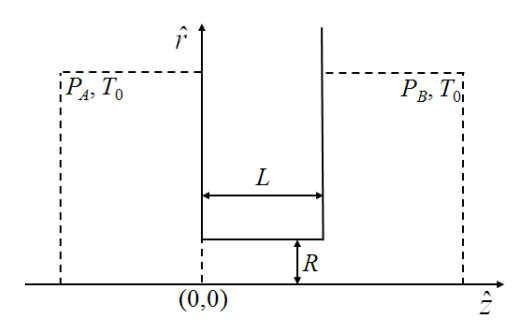


Figure 1: Flow configuration and computational domain.

In the temperature range where the effects of vibrational degrees of freedom can be neglected, the problem may be modelled by the Boltzmann equation for a gas of rigid rotators. The investigation is based on the description of the state of a polyatomic gas using the distribution function  $\hat{f}(\hat{r},\hat{z},\xi,\hat{e})$ , which is a function of the spatial coordinates  $\hat{r}$  and  $\hat{z}$ , the molecular velocity  $\xi$  and the rotational motion energy  $\hat{e}$ . Then, the macroscopic quantities of practical interest are obtained by the moments of the distribution function. Furthermore, it is convenient to introduce the dimensionless independent variables  $z = \hat{z}/R$ ,  $r = \hat{r}/R$  and  $c = \xi/\nu_0$  as well as the dimensionless macroscopic quantities

$$\mathbf{u} = \frac{\hat{\mathbf{u}}}{v_0}, \ e = \frac{\hat{e}}{k_B T_0}, \ f = \frac{\hat{f} v_0^3 \left(k_B T_0\right)^2}{P_A}, \ n = \frac{N k_B T_0}{P_A}, \ p = \frac{P}{P_A}, \ \tau_{tr} = \frac{T_{tr}}{T_0}, \ \tau_{rot} = \frac{T_{rot}}{T_0}, \ T = \frac{3T_{tr} + jT_{rot}}{3 + j}$$
 (2)

where N is the number density, P is the pressure,  $\hat{\boldsymbol{u}}$  is the velocity vector and T is the total (thermodynamic) temperature. The subscripts tr and rot denote the translational and rotational parts, while the parameter j is the number of rotational degrees of freedom (j=0 refers to monoatomic molecules, j=2 to diatomic and linear polyatomic molecules and j=3 to nonlinear polyatomic molecules). The dimensionless flow rate, thrust, impulse factor and discharge coefficient, which are overall quantities of practical interest, are defined respectively as:

$$W = \frac{\dot{M} \nu_0}{\sqrt{\pi} R^2 P_A} = 4\sqrt{\pi} \int_0^1 n_{ex} u_{ex} r dr$$
 (3)

$$F_{t} = \frac{\hat{F}_{t}}{\pi P_{A} R^{2}} = 2 \left[ \int_{0}^{1} \left( 2n_{ex} u_{ex}^{2} + p_{ex} \right) r \, dr \right]$$
 (4)

$$I_{SP} = \frac{\hat{I}_{SP} g_r \sqrt{m}}{\sqrt{2\pi k_B T_0}} = \frac{F_t}{W}$$
 (5)

$$C_{d} = \frac{\dot{M} \, \nu_{0}}{\sqrt{\pi} \, R^{2} \, P_{A} \sqrt{2 \, \pi \, \gamma} \left(\frac{2}{\gamma + 1}\right)^{\frac{\gamma + 1}{2(\gamma - 1)}}} = \frac{W}{\sqrt{2 \pi \, \gamma} \left(\frac{2}{\gamma + 1}\right)^{\frac{\gamma + 1}{2(\gamma - 1)}}}$$
(6)

Here,  $\dot{M}$ ,  $\hat{F}_t$  and  $\hat{I}_{SP}$  are the dimensional mass flow rate, thrust and impulse factor respectively,  $g_r = 9.81 \text{ m/s}^2$  is the gravity acceleration and  $\gamma = (5+j)/(3+j)$  is the ratio of the specific heats of the gas. The subscript ex denotes the values at the exit of the tube (z = L/R). Also, the local Mach number is given by

$$Ma = \frac{|\hat{u}|}{c_s} = \sqrt{\frac{2}{\gamma}} |u| \tag{7}$$

where  $c_s = \sqrt{\gamma k_B T_0/m}$  is the speed of sound and  $|u| = \sqrt{u_r^2 + u_z^2}$  is the magnitude of u.

## 3. Kinetic modelling

The effort of numerically solving the Boltzmann equation is significantly reduced by substituting its collision term with reliable kinetic models. The well-known model introduced by Holway [4] is implemented. The H-theorem can be proved in a straightforward manner for this model following the arguments leading to analogous proof of the BGK model. It is obvious that the dependency of the distribution function  $\hat{f}$  on the energy  $\hat{e}$  of the rotational motion significantly increases the computational effort. However, for the specific problem under consideration the computational effort is reduced by eliminating, based on a projection procedure, the  $\hat{e}$  component of energy by introducing the following reduced distributions [8]:

$$\hat{g} = \int_0^\infty \hat{f} d\hat{e} , \quad \hat{h} = \int_0^\infty \hat{f} \hat{e} d\hat{e}$$
 (8)

Then, for the present flow problem the Holway model may be written in dimensionless form as:

$$c_{p} \cos \theta \frac{\partial g}{\partial r} - \frac{c_{p} \sin \theta}{r} \frac{\partial g}{\partial \theta} + c_{z} \frac{\partial g}{\partial z} = \delta_{0} \rho \sqrt{\tau_{tr}} \left[ \frac{1}{Z} (g_{rot} - g) + \left( 1 - \frac{1}{Z} \right) (g_{tr} - g) \right],$$

$$c_{p} \cos \theta \frac{\partial h}{\partial r} - \frac{c_{p} \sin \theta}{r} \frac{\partial h}{\partial \theta} + c_{z} \frac{\partial h}{\partial z} = \delta_{0} \rho \sqrt{\tau_{tr}} \left[ \frac{1}{Z} (h_{rot} - h) + \left( 1 - \frac{1}{Z} \right) (h_{tr} - h) \right],$$

$$g_{rot} = \frac{n}{(\pi \tau)^{3/2}} \exp \left[ \frac{-(c - u)^{2}}{\tau} \right], \quad h_{rot} = \frac{j \tau n}{2(\pi \tau)^{3/2}} \exp \left[ \frac{-(c - u)^{2}}{\tau} \right],$$

$$g_{tr} = \frac{n}{(\pi \tau_{tr})^{3/2}} \exp \left[ \frac{-(c - u)^{2}}{\tau_{tr}} \right], \quad h_{tr} = \frac{j \tau_{rot} n}{2(\pi \tau_{tr})^{3/2}} \exp \left[ \frac{-(c - u)^{2}}{\tau_{tr}} \right]$$
(9)

Here, the hard-sphere intermolecular potential has been applied. The parameter  $0 < Z^{-1} \le 1$  indicates the rotational collisions as a fraction of the total number of collisions. It is noted, that as the parameter  $Z \to \infty$  the first equation in (9) reduces to the kinetic BGK-model for a monatomic gas [9]. The dimensionless macroscopic quantities are expressed in terms of the functions g and h as:

$$n = \int_{-\infty}^{\infty} \int_{0}^{2\pi} \int_{0}^{\infty} gc_{p}dc_{p}d\theta dc_{z}, \quad u_{r} = \frac{1}{n} \int_{-\infty}^{\infty} \int_{0}^{2\pi} \int_{0}^{\infty} g\left(c_{p}\cos\theta\right)c_{p}dc_{p}d\theta dc_{z}, \quad u_{z} = \frac{1}{n} \int_{-\infty}^{\infty} \int_{0}^{2\pi} \int_{0}^{\infty} gc_{z}c_{p}dc_{p}d\theta dc_{z},$$

$$\tau_{rot} = \frac{2}{jn} \int_{-\infty}^{\infty} \int_{0}^{2\pi} \int_{0}^{\infty} hc_{p}dc_{p}d\theta dc_{z}, \quad \tau_{tr} = \frac{2}{3n} \int_{-\infty}^{\infty} \int_{0}^{2\pi} g\left[\left(c_{p}\cos\theta - u_{r}\right)^{2} + \left(c_{p}\sin\theta\right)^{2} + \left(c_{z} - u_{z}\right)^{2}\right]c_{p}dc_{p}d\theta dc_{z},$$

$$(10)$$

Next, to close the problem the formulation of the boundary conditions is provided. Puerely diffuse boundary reflections are considered at the walls and symmetry is imposed on  $\hat{r} = 0$ . For the open boundaries, a Maxwellian

distribution is supposed based on the local values of the pressure and temperature assuming zero bulk velocity. Based on the above the boundary conditions in dimensionless form can be written as:

Upstream reservoir: 
$$g^{+} = \frac{1}{\pi^{3/2}} \exp(-c^{2}), \quad h^{+} = \frac{j}{2} \frac{1}{\pi^{3/2}} \exp(-c^{2})$$
 (11)

Downstream reservoir: 
$$g^+ = \frac{P_B}{P_A} \frac{1}{\pi^{3/2}} \exp(-c^2)$$
,  $h^+ = \frac{P_B}{P_A} \frac{j}{2} \frac{1}{\pi^{3/2}} \exp(-c^2)$  (12)

Solid walls: 
$$g^+ = \frac{n_w}{\pi^{3/2}} \exp(-c^2)$$
,  $h^+ = \frac{j}{2} \frac{n_w}{\pi^{3/2}} \exp(-c^2)$  (13)

The superscripts (+) denote the outgoing distribution from a surface. The parameter  $n_w$  is calculated by the no penetration condition at the walls. The set of integro-differential Eqs. (9) with the boundary conditions (11-13) are solved numerically discretizing in the physical space by the control volume approach and in the molecular velocity space by the discrete velocity method. The macroscopic quantities are computed by Gauss-Legendre quadrature in the velocity magnitudes and trapezoidal rule in the polar angles. The implemented algorithm has been extensively applied in previous works to solve with considerable success heat transfer configurations [10] and non-linear flows through short tube due to pressure and temperature gradients [11]. The iteration process is terminated when when the convergence criteria

$$\frac{1}{5K} \sum_{i=1}^{K} \left[ \left| \rho_{i}^{(t+1)} - \rho_{i}^{(t)} \right| + \left| \tau_{tr,i}^{(t+1)} - \tau_{tr,i}^{(t)} \right| + \left| \tau_{rot,i}^{(t+1)} - \tau_{rot,i}^{(t)} \right| + \left| u_{z,i}^{(t+1)} - u_{z,i}^{(t)} \right| + \left| u_{r,i}^{(t+1)} - u_{r,i}^{(t)} \right| \right] < \varepsilon$$

$$(14)$$

with t denoting the iteration index and K the number of nodes in the physical space, is fulfilled, while the termination parameter is set to  $\varepsilon = 10^{-9}$ .

### 4. Results and Discussion

Calculations have been carried out in the range of the rarefaction parameter  $\delta_0$  from 0 to 10, i.e. in the free molecular and transition regimes and for L/R=1 and 5. It is noted that typically the parameter Z varies from 1 to 5 and the choice of Z=3 for the problem under question is reasonable. The presented results have been obtained for purely diffuse boundary conditions and the HS model with the upstream and downstream domains being  $15\times15$  unit lengths. Tabulated results are presented for the dimensionless flow rate, thrust, impulse factor and discharge coefficient as well as plotted results for the distribution of various macroscopic quantities.

In Table 1 the dimensionless flow rate W for j=0,2,3 (j=0 refers to monatomic gases) is given. Clearly, the effect of the internal degrees of freedom on the gas flow rate is very small for all values of the rarefaction parameter and for both L/R=1 and 5. It is noted however that for  $\delta_0=1$  and 10, W is decreased as j is increased. Also, W is increased as the length of the channel is decreased and the rarefaction parameter is increased. More specifically, the flow rate for  $\delta_0 \in \left[0.1,1\right]$  increases very slowly and then more rapidly for  $\delta_0 \in \left[1,10\right]$ . Additional simulations have been performed with Z=6 for  $\delta_0=1$  and L/R=1 and 5 showing very small effect on the flow rates.

Table 1: Dimensionless flow rate W in terms of the rarefaction parameter and tube length to radius ratio.

	$\delta_0$								
	0		0.1		1		10		
	L/R = 1	L/R = 5	L/R = 1	L/R = 5	L/R = 1	L/R = 5	L/R = 1	L/R = 5	
j = 0	0.6658	0.3071	0.6781	0.3099	0.7612	0.3344	1.070	0.5487	
j=2	0.6658	0.3071	0.6779	0.3099	0.7598	0.3341	1.053	0.5435	
j=3	0.6658	0.3071	0.6779	0.3099	0.7594	0.3341	1.049	0.5421	

In Table 2 the variation of the dimensionless thrust  $F_t$  in terms of the rarefaction parameter  $\delta_0$  and the ratio L/R is presented. The thrust is increased as the rarefaction parameter  $\delta_0$  is increased and the ratio L/R is decreased. It is clear that the propulsion efficient is increased as the tube length is decreased. Similarly to the flow rates, the rotational degrees of freedom and the parameter Z have a small effect on the values of  $F_t$ . It is seen however, that as j is increased  $F_t$  is slightly increased.

In Table 3 the impulse factor  $I_{sp}$  is shown. As the flow becomes more rarefied,  $I_{sp}$  is decreased. The increment of the rotational degrees of freedom leads to an increment of the impulse factor. This is well expected since the impulse factor is defined as the ration of the thrust over the flow rate with the former one increasing and the latter one decreasing as j is increased.

In Table 4 the discharge coefficient  $C_d$  is presented. The discharge coefficient  $C_d$  decreases by increasing the tube ratio L/R, while for fixed L/R,  $C_d$  is increased as  $\delta_0$  is increased. In addition, as the rotational degrees of freedom are increased from zero to two and then to three, the coefficient  $C_d$  is increased. This is due to the fact that the ratio of the specific heats of the gas is decreased as j is increased, taking also into account that the flow rates of the two types of gases are about the same. Overall it may be concluded that the propulsion characteristics of polyatomic gas expansion through micro-tubes are slightly improved compared with the corresponding ones in the case of monatomic gases.

Table 2: Dimensionless thrust  $F_t$  in terms of the rarefaction parameter and tube length to radius ratio.

	$\delta_0$								
	0		0.1		1		10		
	L/R = 1	L/R = 5	L/R = 1	L/R = 5	L/R = 1	L/R = 5	L/R = 1	L/R = 5	
j = 0	0.4500	0.2079	0.4591	0.2103	0.5215	0.2293	0.7623	0.3867	
<i>j</i> = 2	0.4834	0.2232	0.4925	0.2255	0.5546	0.2442	0.7859	0.4027	
<i>j</i> = 3	0.4918	0.2270	0.5009	0.2293	0.5629	0.2480	0.7922	0.4069	

Table 3: Dimensionless impulse factor  $I_{sp}$  in terms of the rarefaction parameter and tube length to radius ratio.

	$\delta_0$								
	0		0.1		1		10		
	L/R = 1	L/R = 5	L/R = 1	L/R = 5	L/R = 1	L/R = 5	L/R = 1	L/R = 5	
j = 0	0.6759	0.6769	0.6771	0.6786	0.6852	0.6856	0.7124	0.7048	
j=2	0.7260	0.7267	0.7265	0.7275	0.7299	0.7310	0.7463	0.7410	
j=3	0.7386	0.7391	0.7388	0.7398	0.7413	0.7422	0.7552	0.7506	

Table 4: Discharge coefficient  $C_d$  in terms of the rarefaction parameter and tube length to radius ratio.

	$\delta_0$									
	0		0.1		1		10			
	L/R = 1	L/R = 5	L/R = 1	L/R = 5	L/R = 1	L/R = 5	L/R = 1	L/R = 5		
j = 0	0.3658	0.1687	0.3725	0.1703	0.4182	0.1837	0.5879	0.3014		
j = 2	0.3879	0.1789	0.3950	0.1806	0.4427	0.1947	0.6136	0.3167		
<i>j</i> = 3	0.3945	0.1819	0.4017	0.1836	0.4500	0.1980	0.6213	0.3212		

In Figure 2 the distributions of the Mach number along the symmetry axis r=0 for L/R=1 and 5 at  $\delta_0=10$  are shown. The Mach number far upstream is almost zero and is increased in the region just before the tube, while after the tube it is rapidly decreased. It is seen that as the number of the internal degrees of freedom is increased the Mach number is increased due to the decrease of the ratio of the specific heat while the magnitude of the velocity vector in the two types of gas is almost the same.

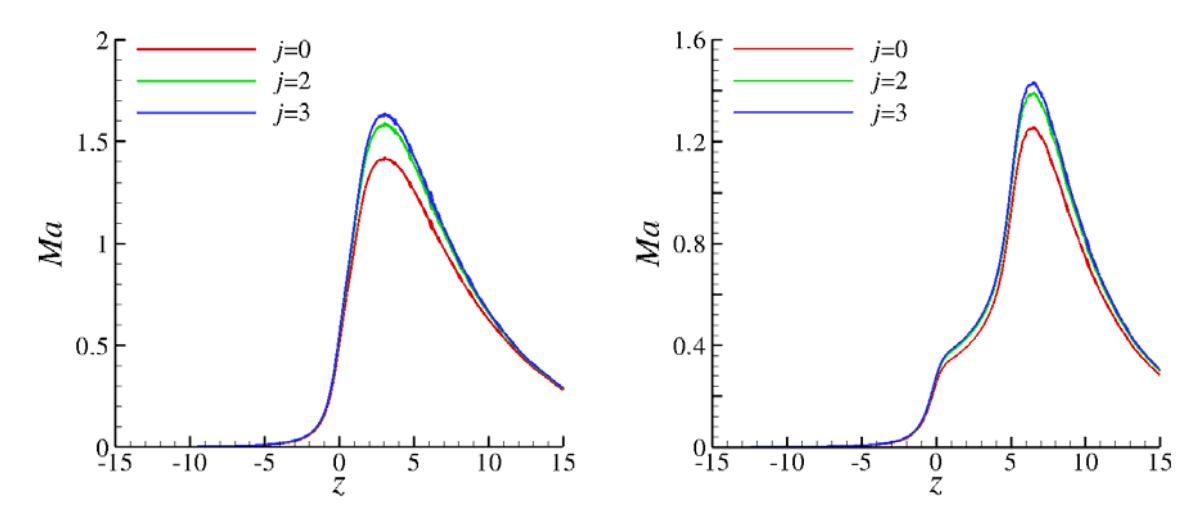


Figure 2: Distributions of the Mach number for L/R = 1 (left) and L/R = 5 (right) with  $\delta_0 = 10$  along the symmetry axis.

In Figure 3 the distributions of the dimensionless axial velocity, pressure, and temperature along the symmetry axis r=0 for  $\delta_0=0.1$  and 10 with L/R=1 are shown. In Figure 4 the corresponding results for L/R=5 are presented. Starting with the pressure variation, it is seen that far upstream is equal to one, then it is rapidly decreased through the tube and finally after the tube it gradually approaches the far downstream conditions. As expected the axial velocity has the same behavior with the Mach number. The maximum value of the velocity is increased as  $\delta_0$  is increased. The axial velocity and the pressure profiles in polyatomic gases (j=2,3) are quantitatively very close to the corresponding profiles for monatomic gases. The temperature equals unity in most of the domain, while inside the tube is decreased. The minimum value of the temperature distribution is decreased as the rarefaction of the gas is decreased and the ratio L/R is increased. In the case of polyatomic gases the translational  $\tau_{tr}$  and total  $\tau_{tot}$  temperatures have the same qualitative behavior with the temperature of the monatomic gas. The rotational temperature  $\tau_{rot}$  is maintained almost constant in the whole domain for small  $\delta_0$ , but as the rarefaction level of the gas is decreased it is also decreased in the same way as the translational and total temperatures.

Distributions of the dimensionless axial velocity and temperatures in the radial direction at the middle (z = L/2R) of the tube are shown in Figure 5 for  $\delta_0 = 1$  and  $\delta_0 = 10$  with L/R = 1. As expected, the velocities have a parabolic type shape with minimum and maximum values at the wall and at the center of the tube, respectively. The velocity profiles of diatomic gases (j = 2) are almost identical with the corresponding monatomic profiles. The corresponding temperature profiles are also shown. In all cases a temperature drop across the tube (radial direction) is observed. For  $\delta_0 = 1$ , the translational temperature of a diatomic gas is close to the corresponding temperature of a monatomic gas, while the rotational temperature is kept almost constant. For  $\delta_0 = 10$ , the translational temperature of a diatomic gas is higher than the temperature of a monatomic gas, while the rotational temperature is not constant anymore and it is reduced moving from the wall towards the center of the tube.

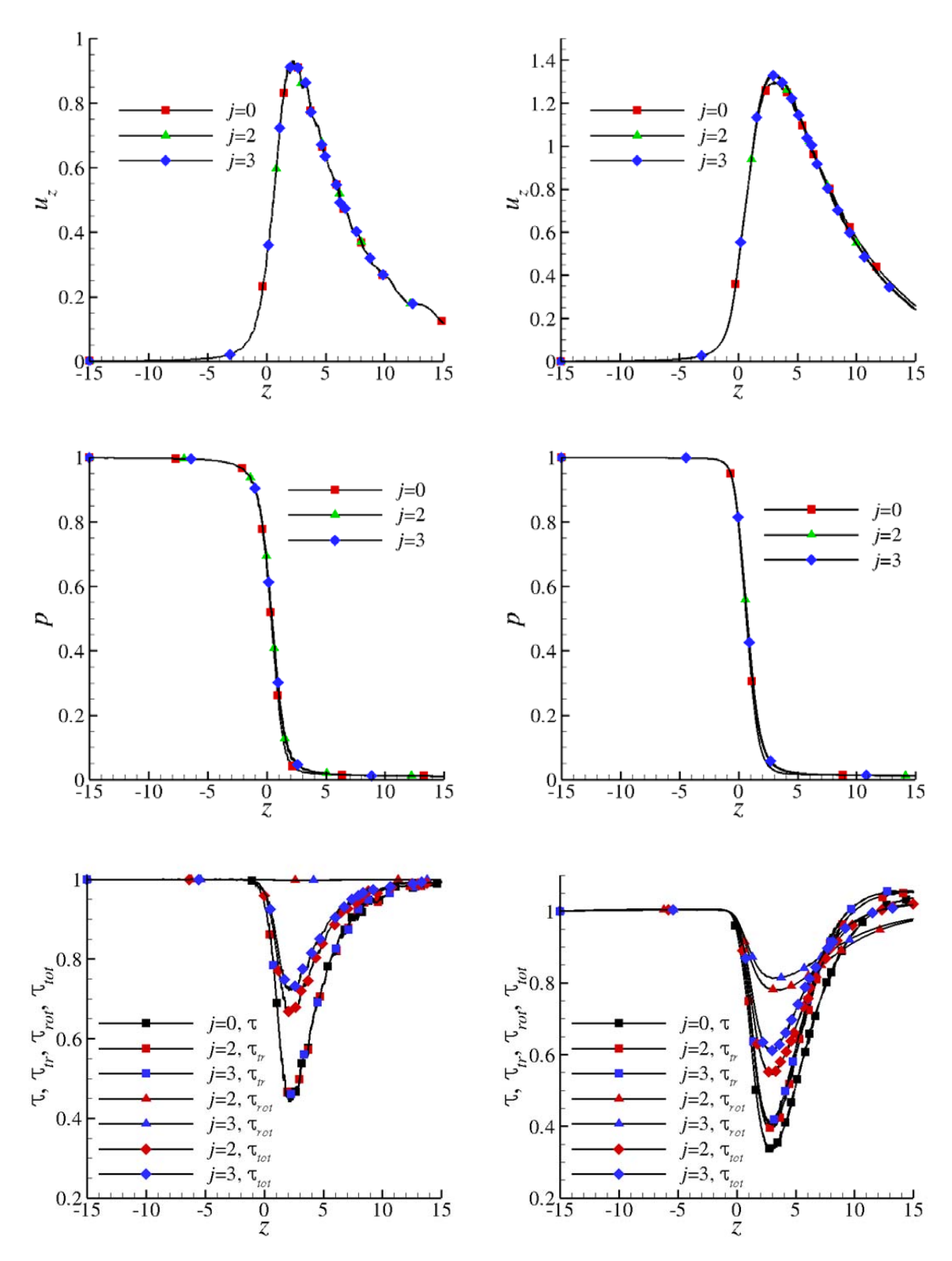


Figure 3: Dimensionless distributions of axial velocity (up), pressure (middle) and temperatures (down) for  $\delta_0=0.1$  (left) and  $\delta_0=10$  (right) with L/R=1 along the symmetry axis.

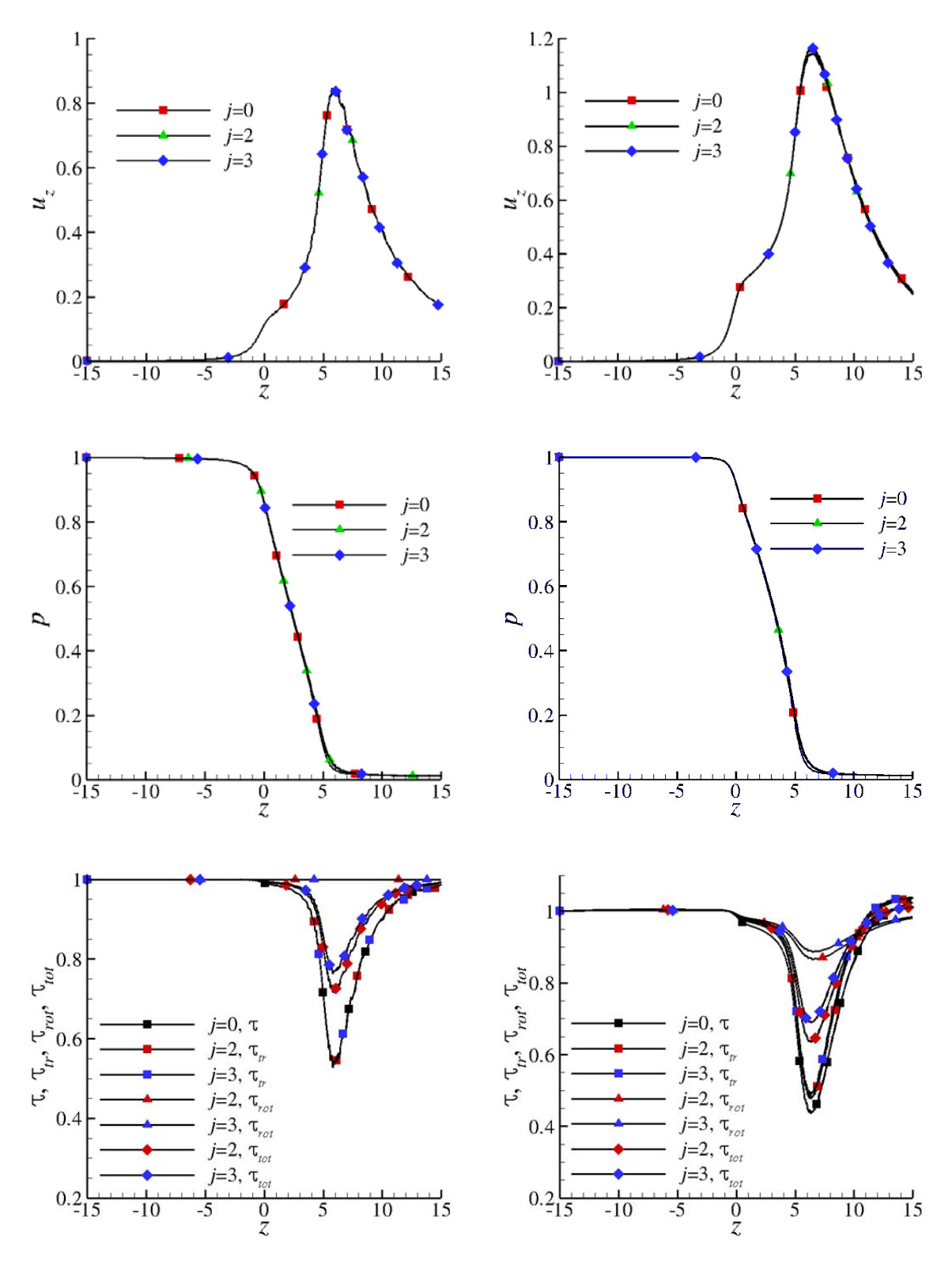


Figure 4: Dimensionless distributions of axial velocity (up), pressure (middle) and temperatures (down) for  $\delta_0=0.1$  (left) and  $\delta_0=10$  (right) with L/R=5 along the symmetry axis.

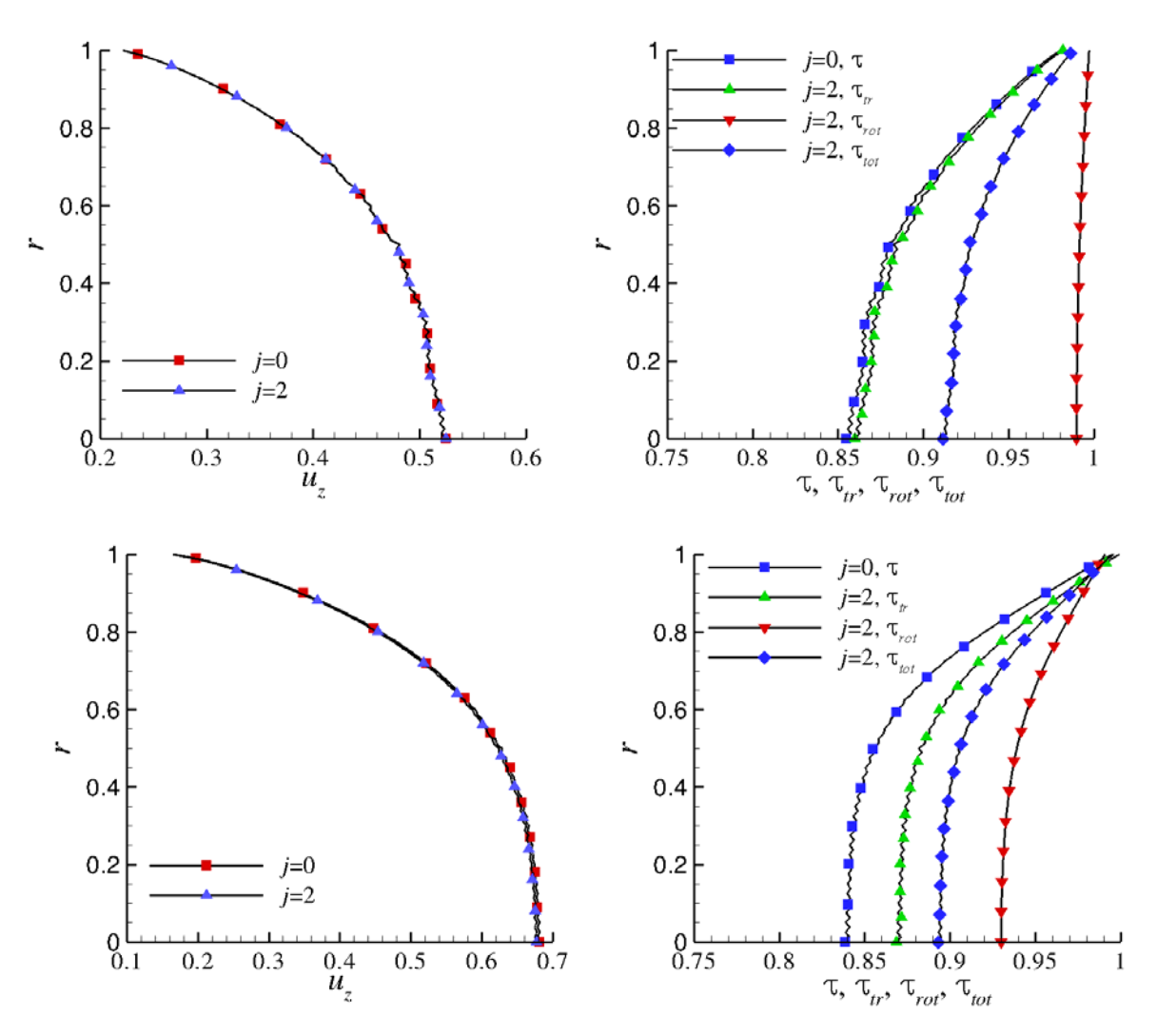


Figure 5: Distributions of axial velocity (left) and temperatures (right) for  $\delta_0 = 1$  (up) and  $\delta_0 = 10$  (down) with L/R = 1 at z = L/(2R).

#### 5. Conclusion

The characteristic parameters of short tubes operating as propulsion systems in the case of polyatomic gases have been computed implementing kinetic modeling. Solving the Holway kinetic model subject to diffuse boundary conditions the flow rate, the thrust, the impulse factor and the discharge coefficient as well as the distributions of the macroscopic quantities with practical interest have been obtained. It is found that the effect of the rotational degrees of freedom on the macroscopic quantities is small except in the case of temperature distributions. It may be concluded that the overall propulsion efficiency in the case of polyatomic gases compared to the one in monatomic gases is slightly improved. In addition it has been demonstrated that polyatomic kinetic modeling may be applied as an alternative approach to DSMC. The implemented parametric study may be useful in optimizing the design and manufacturing of micro-nozzles applied in micro-propulsion systems under rarefied conditions.

#### References

- [1] Lilly, T. C., S. F. Gimelshein, A. D. Ketsdever, and G. N. Markelov. 2006, Measurements and computations of mass flow and momentum flux through short tubes in rarefied gases, *Phys. Fluids*, 18:093601.
- [2] Varoutis, S., D. Valougeorgis and F. Sharipov. 2009, Gas flow through tubes of finite length over the whole range of rarefaction for various pressure drop ratio, *J. Vac. Sci. & Technol. A*, 27:1377-1391.

- [3] Misdanitis, S., S. Pantazis and D. Valougeorgis. 2012, Pressure driven rarefied gas flow through a slit and an orifice, *Vacuum*, 86:1701-1708.
- [4] Holway, L. H. 1966, New statistical models for kinetic theory: Methods of construction, *Phys. Fluids*, 9:1658-1673.
- [5] Tantos, C., D. Valougeorgis, M. Pannuzzo, A. Frezzotti and G. L. Morini. 2014, Conductive heat transfer in a rarefied polyatomic gas confined between coaxial cylinders, *Int. J. Heat Mass Tran.*, 79:378-389.
- [6] Tantos, C., D. Valougeorgis and A. Frezzotti. 2015, Conductive heat transfer in rarefied polyatomic gases confined between parallel plates via various kinetic models and the DSMC method, *Int. J. Heat Mass Tran.*, 88:636-651.
- [7] Frezzotti, A. and T. Ytrehus. 2006, Kinetic theory study of steady condensation of a polyatomic gas, *Phys. Fluids*, 18:027101-11-12.
- [8] Andries, P., J.F. Bourgat, P. Tallec, B. Perthame. 2002, Numerical comparison between the Boltzmann and ES-BGK models for rarefied gases, *Comput. Methods Appl. Mech. Eng.*, 191:3369–3390.
- [9] Bhatnagar, P. L., E. P. Gross, and M. A. Krook. 1954. A model for collision processes in gases. I. Small amplitude processes in charged and neutral one-component systems. *Phys. Review*, 94:511-525.
- [10] Pantazis, S. and D. Valougeorgis. 2010, Non-linear heat transfer through rarefied gases between coaxial cylindrical surfaces at different temperatures, *Eur. J. Mech. B-Fluid*, 29:494-509.
- [11] Pantazis, S., S. Naris, C. Tantos, D. Valougeorgis, J. Andre, F. Millet and J. P. Perin. 2013, Nonlinear vacuum gas flow through a short tube due to pressure and temperature gradients, *Fusion Eng. Des.*, 88:2384-2387.